Available online at www.sciencedirect.com

SciVerse ScienceDirect

Ceramics International 38 (2012) 5575–5583

CERAMICS INTERNATIONAL

www.elsevier.com/locate/ceramint

Temperature dependent synthesis and optical properties of CdSe quantum dots

Wen Mi, Jintao Tian *, Weiguo Tian, Jinhui Dai, Xin Wang, Xiaoyun Liu

Institute of Materials Science and Engineering, Ocean University of China, Songling Road 238, Qingdao 266100, PR China

Received 27 February 2012; accepted 31 March 2012
Available online 24 April 2012

Abstract

The CdSe quantum dots (QDs) were synthesized at various temperatures in aqueous solution. The as-synthesized QDs were characterized by X-ray diffraction (XRD) method and transmission electron microscopy (TEM), and their optical properties were assessed via ultraviolet–visible (UV–vis) absorption spectrum and fluorescence spectrum. The results showed that the reaction temperature could significantly influence the band gap, particle size, and spectral behaviors of the QDs. With the increase of the temperature from room temperature to 90 °C, the band gap of the QDs linearly decreased, corresponding to an essential increase of particle size as well as variable spectral behaviors. In particular, the starting temperature had an important effect on the QDs synthesis and their optical properties. From a viewpoint of wide controls of fluorescence color and intensity, a reaction temperature range of 17–90 °C was appropriate for the synthesis of the CdSe QDs.

Keywords: C. Optical properties; CdSe; Quantum dots; Temperature

1. Introduction

In the past decade, zero dimensional semiconductor nanomaterials have attracted great interest owing to the unique optical and electrical properties, and have been used in immunoassay, cell imaging, body imaging, disease diagnosis, and other biological fields [1]. When the size of a semiconductor is less than its first Bohr radius, the nanoparticles are generally called quantum dots (QDs) and quantum confinement effects appeared such as raise in the band gap, E_g, and blue shifts of the adsorption and fluorescence spectra [2–5]. Cadmium selenide (CdSe) is one of the most important semiconductors having direct band gap of 1.74 eV [6]. For CdSe QDs, the band gap can be tuned to cover the whole visible range by varying the crystallite size [7]. Its well controllable photoluminescence property along with stability and narrow emission bandwidths has made them potential candidates in light-emitting diodes (LEDs) [8–10], solar cells [11,12], and biological labeling [13–15]. Recent developments in preparations of colloidal QDs can allow many sophisticated nanostructures like core/shell heterostructures [16,17]. Since the optical performances of the coated CdSe QDs mainly depend on the CdSe core, the preparation of the CdSe core is quite crucial. Currently, two synthetic routes, i.e. organic-phase and aqueous-phase approaches, have been proposed to produce CdSe QDs with desired optical properties for the biomedical research and applications. The synthesized QDs from organic-phase approach are insoluble in an aqueous solution and therefore are not compatible with the biological system while the aqueous synthesis is reagent-effective, less toxic and more reproducible which improves the water-stability and biological compatibility [18]. Thus, much effort has been paid on the synthesis of II-VI semiconductor QDs such as CdS [19], ZnS [20], CdSe [21], and CdTe [22] in aqueous solutions, though the qualities of the synthesized QDs were not quite good and further work was yet to conduct. Since the emission color of semiconductor nanocrystals is strongly dependent on size [23] and shape [24], the color purity of the emission becomes dependent on the size and shape distribution of a nanocrystal sample. Therefore, the control of the emission color and color purity is likely a matter of the control of the size/shape and size/shape distribution of the semiconductor nanocrystals, regarding which the recent studies have provided a reasonable knowledge basis [25–28]. The major factors for CdSe synthesis in aqueous

* Corresponding author. Tel.: +86 532 66781690; fax: +86 532 66781320.
E-mail address: jttian@ouc.edu.cn (J. Tian).

0272-8842/$36.00
http://dx.doi.org/10.1016/j.ceramint.2012.03.077

solution are reaction temperature, reaction time, reactant ratio, pH value of the solution, stabilizer and its amount, etc. Since the reaction temperature plays a major role in determining nucleation and growth of the CdSe nanocrystals, it is of great importance to study the influence of reaction temperature on the QDs synthesis. In this study we would like to conduct a temperature dependent synthesis of CdSe QDs. A wide temperature range of 17–90 °C were applied. The as-synthesized QDs were characterized and their optical properties were examined.

2. Experimental procedure

2.1. Raw materials

Several chemicals of cadmium chloride ($CdCl_2{\cdot}2.5H_2O$), thioglycollic acid ($HSCH_2COOH$, TGA), sodium hydroxide (NaOH), selenium (Se) powder, sodium borohydride ($NaBH_4$) were used in this study. All of them were of analytical grade and used as received without any further purification. All aqueous solutions were prepared with deionized water.

2.2. Preparation of the CdSe QDs

In this study the CdSe QDs were synthesized via aqueous-phase approach. The CdSe nanocrystals were formed by directly mixing of a Cd source solution containing Cd^{2+} and a Se source solution containing sodium hydrogen selenide (NaHSe). The NaHSe was obtained from a reaction occurred between $NaBH_4$ and Se powder. In a typical synthesis, the involved solutions were prepared as below. 0.012 g Se powder and 0.012 g $NaBH_4$ were added to 100 mL deionized water under nitrogen atmosphere to form a black mixture. The mixture was continuously stirred under nitrogen until the black color disappeared. The Se source solution containing NaHSe was then obtained [29]. 0.069 g $CdCl_2{\cdot}2.5H_2O$ and 0.07 mL TGA were dissolved in 170 mL deionized water to form a Cd source solution and its pH value was adjusted to 11 by using a 1.0 M NaOH solution. The solution was then deoxygenated by bubbling nitrogen for at least 30 min.

The CdSe QDs synthesis was conducted in a three-neck flask. The instrument and the proposed temperature increasing procedure were shown in Fig. 1. Firstly, the Cd source solution was placed in a flask and bubbled at room temperature of 17 °C with nitrogen for at least 30 min. After that, some amount of the freshly prepared NaHSe solution was poured into the flask under nitrogen atmosphere. The CdSe crystal nuclei were immediately formed, accompanied by a color change from colorless to very light green. The molar ratio of chemicals in the final solution was kept to be Cd^{2+}/Se^{2-}/TGA of 2/1/6. After being stirred at 17 °C for 30 min, 25 mL solution was taken as a sample from the flask with a pipette and conserved in a nitrogen filled brown bottle (S_1 in Fig. 1b). The temperature was then increased to 30 °C, 50 °C, 70 °C, and 90 °C in an orderly fashion. At each temperature stage reaction time of 30 min was applied and 25 mL solution was taken as a sample (S_2–S_5). For temperature of 90 °C, another 30 min was applied and S_6 was obtained.

2.3. Characterization and measurements

The X-ray diffraction (XRD) patterns of the CdSe QDs powder samples were obtained from a German Bruker D8 Advance X-ray diffractometer. The transmission electron microscopy (TEM) image and the selected area electron diffraction (SAED) patterns were recorded on a JEM-2100 Japan JEOL electron microscope. The ultraviolet–visible (UV–vis) absorption spectra were recorded with a U-3010 Hitachi spectrophotometer. The fluorescence spectra were obtained using a Fluorolog 3-P spectrofluorometer (Jobin Yvon).

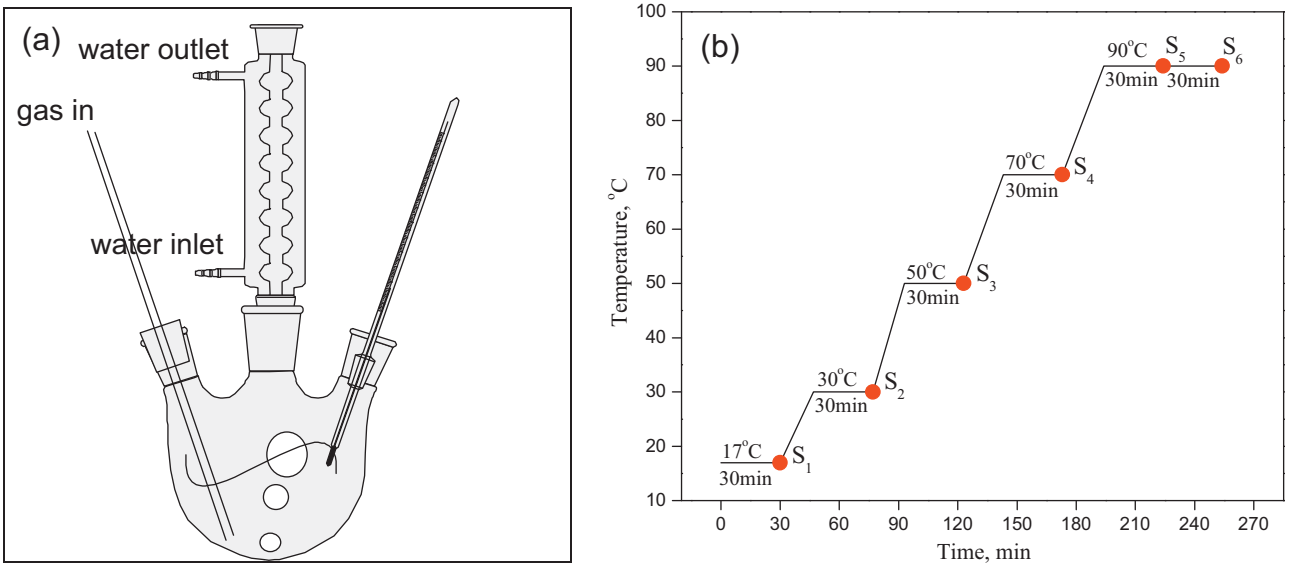

Fig. 1. Schematic illustration of the experimental instrument for temperature dependent CdSe QDs synthesis (a) and the proposed temperature increasing procedure (b). By applying a reaction time of 30 min for each temperature stage, totally six samples of S_1–S_6 were taken for measurements.

3. Results and discussion

3.1. XRD patterns

The CdSe QDs were synthesized over a wide temperature range of 17–90 °C in aqueous solution. The as-synthesized QDs were isolated from solutions using a centrifuge and dried to be powders in a vacuum oven at a temperature below 40 °C. The powders were then characterized by XRD method and the results were shown in Fig. 2. Besides, an XRD examination of a coarse CdSe particles from a direct precipitation was also conducted and incorporated in this figure for comparison. As seen from Fig. 2, the coarse CdSe had three strong diffraction peaks with visible broadening. These peaks corresponded well with a cubic CdSe phase (JCPDS No. 19-0191, vertical bars at the bottom of the figure). In the cases of the CdSe QDs, however, no visible strong diffraction peak was observed. Broad humps existed at 2θ values of 27.3° and 45.8° for all the CdSe samples (S_1–S_6), suggesting a rather small particle size of the QDs. The humps at 45.8° were supposed to be a result of the integration of the peak$_{(2\ 2\ 0)}$ and peak$_{(3\ 1\ 1)}$. Similar appearance has been presented in Ref. [21], where with an increase of the Scherrer size from 1.7 nm to 2.1 nm a segregating process of a hump to peaks was observed. It should be noted that in Fig. 2 a non-ignorable 2° shift of the humps toward large angle has been definitely obtained, compared to that of the coarse CdSe. Although we could not give a sound explanation up to now, grain imperfection of the QDs due to their very small size would probably play a crucial role for such shift. In fact, the QDs had a Scherrer size as small as 0.8–1.2 nm (see data in Table 1) that were from the famous Scherrer equation of [30]

$$D_c = \frac{k\lambda}{\sqrt{B^2 - B_S^2}\cos\theta} \quad (1)$$

where D_c was the average particle diameter, k was a shape factor of the particle (normally chosen as 0.89), λ was the wavelength of X-ray in nanometer (0.1541 nm for Cu K_α in this study), B was the peak FWHM (full width at half maximum) of the QDs samples, B_s was the instrument induced peak FWHM that has been determined to be 0.244° with a well crystallized coarse Al_2O_3 powder in this study, and θ was the incident angle of X-ray, respectively. Although the Scherrer size data in Table 1 were comparable to each other and did not show an increasing tendency, the more broadening patterns in Fig. 2 revealed a particle size of the QDs in this study essentially smaller than those in Ref. [21].

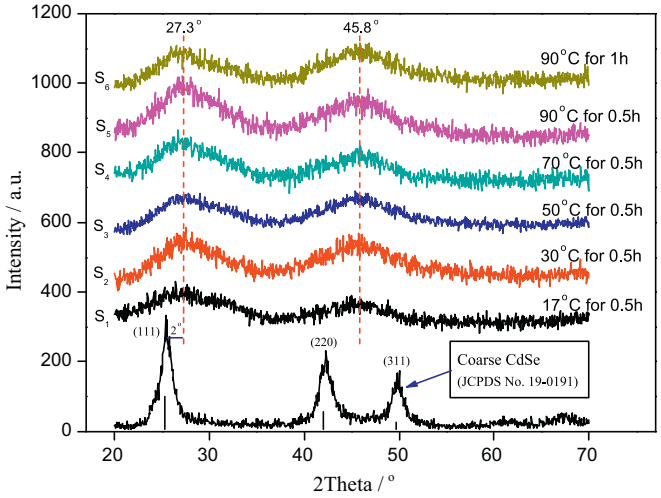

Fig. 2. XRD patterns of the CdSe QDs synthesized at various temperatures.

3.2. TEM observation

The CdSe QDs synthesized over a temperature range of 17–90 °C were physically color gradient, as shown in Fig. 3a. The QDs in solution obtained at room temperature of 17 °C were pale green and then became light green and green with the raise of the reaction temperature to 30 and 50 °C. The QDs synthesized at 70 °C was not green but light yellow, suggesting a substantial change of the particles at this temperature. With a continuous increase of the temperature to 90 °C and another 30 min delay of the reaction time the S_5 and S_6 samples were yellow and orange. Similar color gradient was observed for the powder samples. This suggested that the reaction temperature had an essential effect on the CdSe QDs. The direct observation of the QDs was conducted through TEM and a typical image was shown in Fig. 3b. Here only the QDs synthesized at 17 °C (S_1) were selected for TEM observation for an economic intention. As seen, the QDs synthesized in this study consisted of basically round particles. Most of these particles were of 2–3 nm. The diameter of the QDs from TEM observation was therefore almost three times of the Scherrer size (see data in Table 1), in agreement with a common consequence that the

Table 1
Particle size estimations of the CdSe QDs synthesized in this study.

Reaction condition	Peak position (nm)	E_g^{*op} (eV)	Diameter from models			Diameter from measurements	
			Brus [3]	Peng [36]	Bacherikov [37]	XRD	TEM
17 °C for 0.5 h	388.5	2.92	3.35	1.45	0.98	0.83	2–3
30 °C for 0.5 h	394	2.89	3.39	1.50	1.03	1.08	–
50 °C for 0.5 h	429	2.71	3.67	1.79	1.34	1.01	–
70 °C for 0.5 h	436	2.61	3.86	1.85	1.42	1.04	–
90 °C for 0.5 h	454.5	2.51	4.09	1.98	1.64	1.09	–
90 °C for 1 h	452	2.50	4.11	1.97	1.61	1.21	–

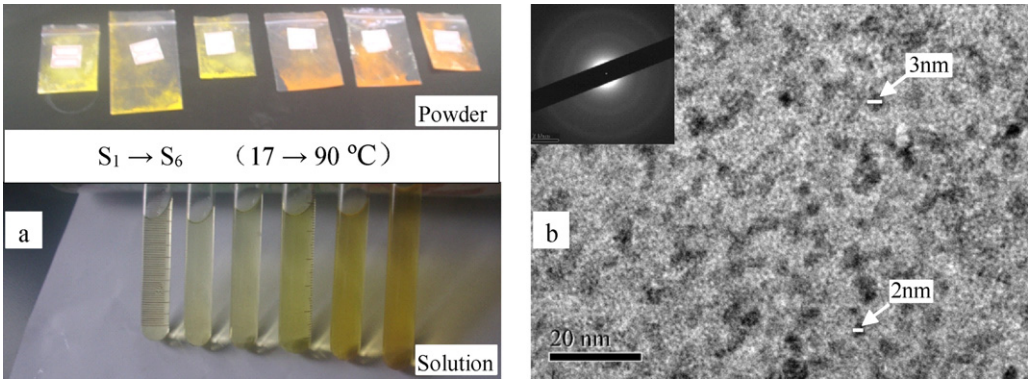

Fig. 3. Observations of the CdSe QDs synthesized at various temperatures from naked eye (a) and TEM (b). The selected area electron diffraction (SAED) patterns of the QDs were also incorporated in this figure.

particle size from TEM image was generally larger than that from XRD patterns. The selected area electron diffraction (SAED) patterns of the QDs were also shown in Fig. 3b. Two concentric rings were observed, giving interplanar distances of 0.332 and 0.203 nm. Note that there had three diffraction peaks at 25.3°, 42.0°, and 49.7° for the coarse CdSe and the corresponded interplanar distances were 0.351, 0.215, and 0.183 nm while in the cases of the QDs only two humps were observed at 27.3° and 45.8° with interplanar distance of 0.326 and 0.198 nm (see Fig. 2). Thus the TEM and SAED results of the QDs were in good agreement with those of the XRD patterns and confirmed again the non-ignorable 2° shift. Another interesting point was that the two concentric rings in Fig. 3b were visibly broadened, a sign of interplanar distance distribution of the QDs. Thus, the rather flat humps in Fig. 2 was related probably not only to the particle refinement but also to the interplanar distance distribution of the QDs.

3.3. UV–vis spectra

UV–vis absorption spectroscopy is a very common analytical tool used in the characterization of CdSe QDs as the lowest energy absorption feature (the first exciton) and can yield information on the band gap, particle size, and size dispersion [28]. Here we would like to firstly give a rough illustration of band gap determination from a UV–vis spectrum. Fig. 4 shows a typical UV–vis spectrum from our experiments. A typical absorption peak ($Peak_{II}$) and an absorption shoulder ($Peak_{III}$) were clearly observed in Fig. 4a. Band edge positions could be determined by finding the local minimums of the derivative curve of the absorption spectrum, as labeled by BD_{II} and BD_{III} in this figure. With this band edge position a tangent line was made and its intersection with x-axis (Abs = 0) led to the determination of λ_{onset} [31]. This λ_{onset} was generally a sign of optical absorption onset. By introducing a rough formula of $E_g = 1240/\lambda$, the λ_{onset} corresponded to an optical absorption band gap (E_g^{*op}). Another method for determination of E_g^{*op} was from the equation of [32]

$$a(h\nu) = A(h\nu - E_g^*)^{1/2}, \quad (h\nu \geq E_g^*) \tag{2}$$

where $h\nu$ was photo energy, a was the absorption coefficient, A was the constant, and E_g^* was the band gap of the nanoparticles. By applying the above equation to the absorption spectrum, a relationship curve of $[a(h\nu)]^2$ against $h\nu$ was shown in Fig. 4b. An inflection point upon this curve could be fixed by finding the

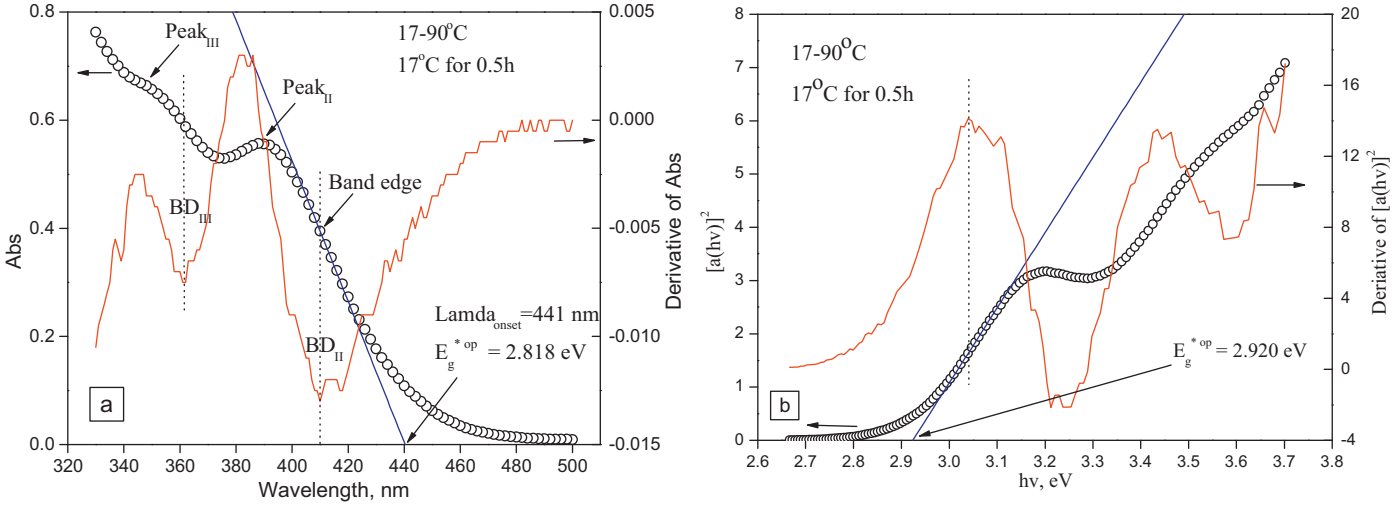

Fig. 4. Optical absorption band gap determination from (a): λ_{onset}; (b): Eq. (2). The CdSe QDs sample was synthesized at 17 °C. Details for λ_{onset} and Eq. (2) were given in the text.

maximum of the derivative curve of the relationship curve. The tangent line through this inflection point intersected with x-axis ($[a(h\nu)]^2 = 0$) and gave the value of E_g^{*op}. With the two methods described above, E_g^{*op} values of 2.818 eV and 2.920 eV were separately obtained for the CdSe QDs sample synthesized at 17 °C. They were much larger than that of the bulk CdSe (1.74 eV). The calculated blue shift was as much as ~270 nm. The particle size of the CdSe nanocrystals was therefore rather small. It should be noted that the E_g^{*op} value from the λ_{onset} was slightly smaller than that from Eq. (2). The disparity was 3.5%.

The UV–vis absorption spectra of the colloid CdSe QDs obtained at a temperature range of 17–90 °C were shown in Fig. 5a. Three absorption regions with absorption peaks were clearly observed, as labeled by $Peak_I$, $Peak_{II}$, and $Peak_{III}$ in the figure. The peak positions, however, were noticeably changed with the reaction temperature. Red shifts were observed with the raise of reaction temperature. The wavelength of the first exciton (the first long wavelength absorption peak) for the 17 °C sample (S_1) was 388 nm while in the case of the 90 °C sample (S_5) it was 454 nm. The resultant red shift of the first exciton was as high as 66 nm. Thus, an increasing tendency of the particle size with the reaction temperature was concluded for the CdSe QDs. Besides, the peak intensities and shapes also evidently varied with the temperature in Fig. 5a. Generally, a sharp absorption peak with high intensity and low FWHM implied homogeneous nanoparticles with narrow particle size distribution [33]. The results in Fig. 5a revealed a wide particle size distribution for the CdSe QDs nanoparticles due to the raise of the reaction temperature. In fact, such results could be visibly understood from the derivative curves shown in Fig. 5b. As described in Fig. 4a, the band edge position of an absorption peak could be determined by finding the local minimum of the derivative curve of the absorption spectrum. The band edge positions for those peaks in Fig. 5a have been labeled with BD_I,

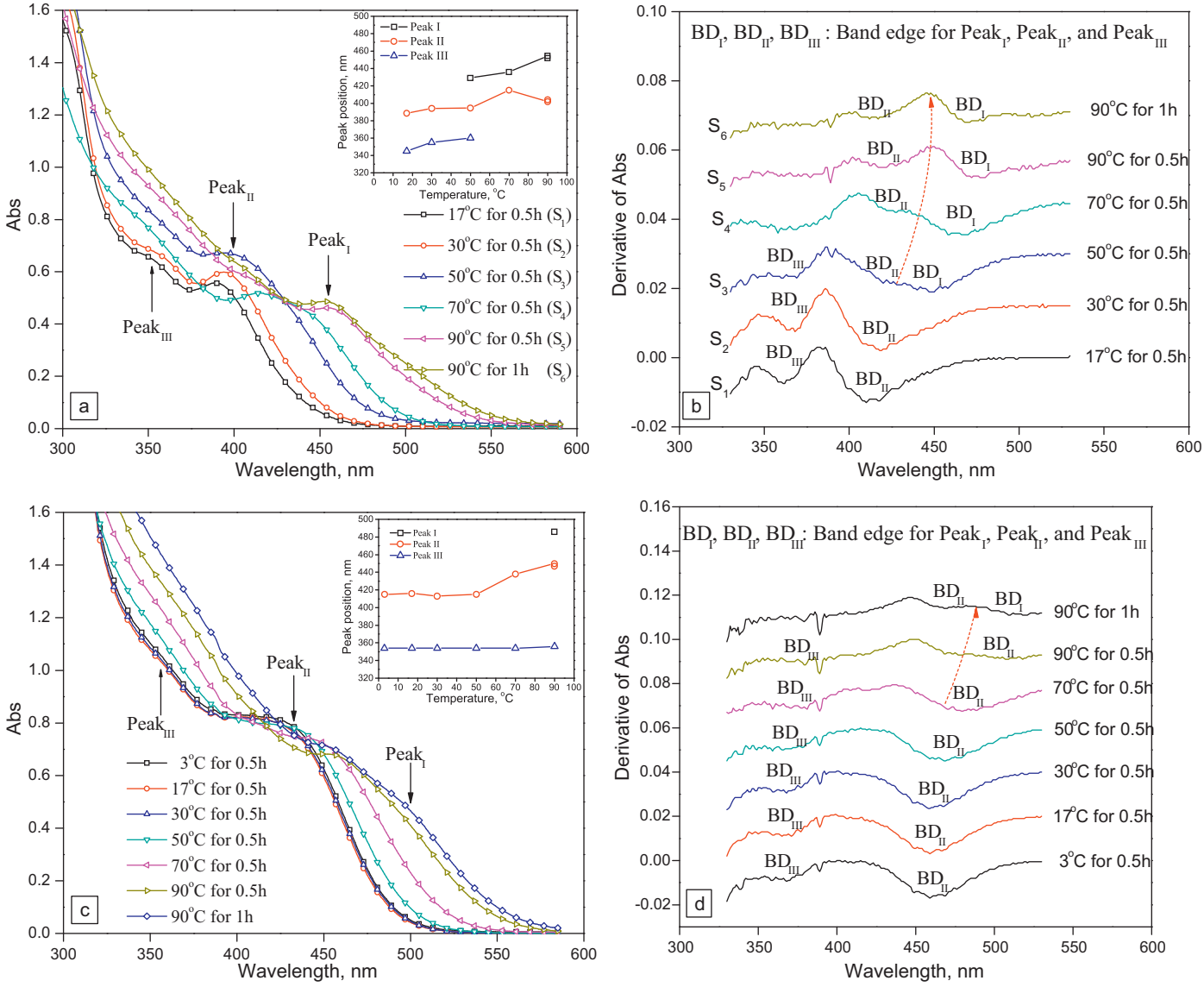

Fig. 5. UV–vis absorption spectra of the colloid CdSe QDs obtained at temperature ranges of 17–90 °C (a) and 3–90 °C (c). The derivative curves of the absorption spectra were shown in this figure (b and d), respectively.

BD_{II}, and BD_{III} in Fig. 5b. As seen, derivative curves for the 17 and 30 °C samples were quite uneven with large crest and trough. With the raise of reaction temperature to 50 °C, both the crest and trough became small. In particular, a very small wave crest was observed (initial point of the dotted arrow in Fig. 5b). This small crest was a sign of the appearance of a new absorption peak. With the reaction temperature increased to 70 and 90 °C, this small crest gradually grew up while the whole derivative curves became flat. The growing process of the crest was clearly marked out with a dotted arrow in Fig. 5b. Since a UV–vis spectrum containing a sharp absorption peak mathematically corresponded to an uneven derivative curve with large crest and trough, the behavior of the derivative curve at each temperature in Fig. 5b coincided well with the peak features in Fig. 5a. From this point of view, the method shown in Fig. 5b is a good tool to visibly understand the peak feature for a UV–vis spectrum.

Beginning to react from 17 °C, Fig. 5a showed a peak position with a rather low wavelength of 388 nm for the first exciton and a large red shift of 66 nm due to the temperature increase. We supposed that the initial reaction temperature may also affect the CdSe QDs synthesis to some extent. So a rather low starting temperature of 3 °C was applied and the UV–vis spectra of the resultant CdSe QDs were shown in Fig. 5c. As seen from Fig. 5c, the absorption spectra scarcely changed with the raise of the temperature from 3 °C to 30 °C. The wavelength of the first exciton for the 3 °C sample was 415 nm, larger than that of the 17 °C sample (Fig. 5a, 388 nm). The CdSe nanoparticles grew hardly at this temperature range. With the temperature continuously increased to 50 °C, 70 °C, and 90 °C, red shifts were observed and the final value were moderate (35 nm). In fact, the spectra in Fig. 5c were not altered as much as those in Fig. 5a due to the raise of the reaction temperature. Not absorption peaks but shoulders appeared at this temperature range near the long wavelength. This could be visibly understood by comparing the derivative curves in Fig. 5d with those in Fig. 5b. The curves in Fig. 5d were quite flat, compared to those in Fig. 5b. The new peaks were incubated from 70 °C, larger than that of 50 °C in Fig. 5b. The above results demonstrated that the initial reaction temperature had a strong effect on the synthesis of the CdSe QDs and their optical properties. A moderate starting temperature, for instance 17 °C in this study, was helpful to the CdSe QDs formation with a narrow particle size distribution and accordingly a obvious UV–vis absorption peak.

3.4. Optical band gap and particle size

The optical absorption band gap, E_g^{*op}, of the CdSe QDs could be experimentally determined from the UV–vis spectra. By applying the two methods shown in Fig. 4a and b, the E_g^{*op} values from the UV–vis spectra in Fig. 5a and c were shown in Fig. 6a. As seen from Fig. 6a, linear decreasing tendencies were obtained for the E_g^{*op} over a temperature range of 17–90 °C. The E_g^{*op} values from the λ_{onset} method were slightly smaller than those from Eq. (2), giving an average discrepancy of 0.12 eV. Since the results from Eq. (2) were more true to reflect the real situation of the QDs, a linear fitting to these data (solid circles in Fig. 6a) gave a relationship of

$$E_g^{*op} = [3.05 - 0.0062T] \quad (3)$$

where E_g^{*op} was the optical absorption band gap in eV and T was the temperature in °C. In the case of the temperature range of 3–90 °C, all the E_g^{*op} values were smaller than those of the 17–90 °C range. The E_g^{*op} changed little at low temperatures (3–30 °C), then decreased to some extent over 30–50 °C, and finally decreased linearly at high temperatures (50–90 °C). The derived discrepancy was 0.10 eV.

Since the band gap of nanoparticle was closely related to its particle size, the diameter of the CdSe QDs synthesized in this study was estimated by using the famous Brus effective mass approximation model with a formula of [3]

$$\Delta E_g = E_g^* - E_g \approx \frac{h^2}{8R^2}\left[\frac{1}{m_e^*} + \frac{1}{m_h^*}\right] - \frac{1.8e^2}{\varepsilon R} \quad (4)$$

where ΔE_g was the energy of the first excited state, E_g^* and E_g were the nanoparticle and bulk band gaps (E_g of 1.74 eV for CdSe), h was the Planck's constant, ε was the dielectric constant, R was the radius of the nanoparticle, e was the elementary charge, m_e^* and m_h^* were the effective masses of electron and hole, respectively. With the essential data from Ref. [34], the estimated diameters from Eq. (4) were summarized in Table 1 and plotted in Fig. 6b. As seen, increasing tendencies were obtained for the diameters of the CdSe nanoparticles. With a starting temperature of 17 °C, the CdSe nanoparticles linearly grew up with a raise of temperature from 17 °C to 90 °C. The derived diameter range were of 3.35–4.11 nm. A diameter discrepancy of 0.31 nm was observed. In the cases of the samples started from 3 °C, the derived diameters were quite large. The nanoparticles at low temperatures (3–30 °C) were much larger than those of the 17–90 °C samples and scarcely changed. For high temperatures (50–90 °C) they were linearly grown up. The size discrepancy in this case was 0.28 nm. Note that the TEM observations gave a particle size of 2–3 nm for the QDs, the diameter results from Eq. (2) (solid symbols in Fig. 6b) were more true to reflect the real situation of the QDs than those from λ_{onset} (open symbols in Fig. 6b). From this point of view, the method given in Fig. 4b was more accurate and suitable for the determination of the band gap as well as particle size than that in Fig. 4a.

In fact, the theoretical estimation of the CdSe diameter from the Brus effective mass approximation model was quite rough [23,35]. Two empirical equations have been proposed by some researchers [36,37]:

$$D = (1.6122 \times 10^{-9})\lambda^4 - (2.6575 \times 10^{-6})\lambda^3 + (1.6242 \times 10^{-3})\lambda^2 - (0.4277)\lambda + (41.57) \quad (5)$$

$$D = 0.344e^{(\lambda - 252.7)/129.3} \quad (6)$$

where D (nm) was the size of nanocrystals and λ (nm) was the wavelength of the first excitonic absorption peak of the corresponding sample. With these empirical formulas, the particle sizes of the QDs were calculated and summarized in Table 1. The relationship between E_g^{*op} and diameter were plotted in Fig. 6c.

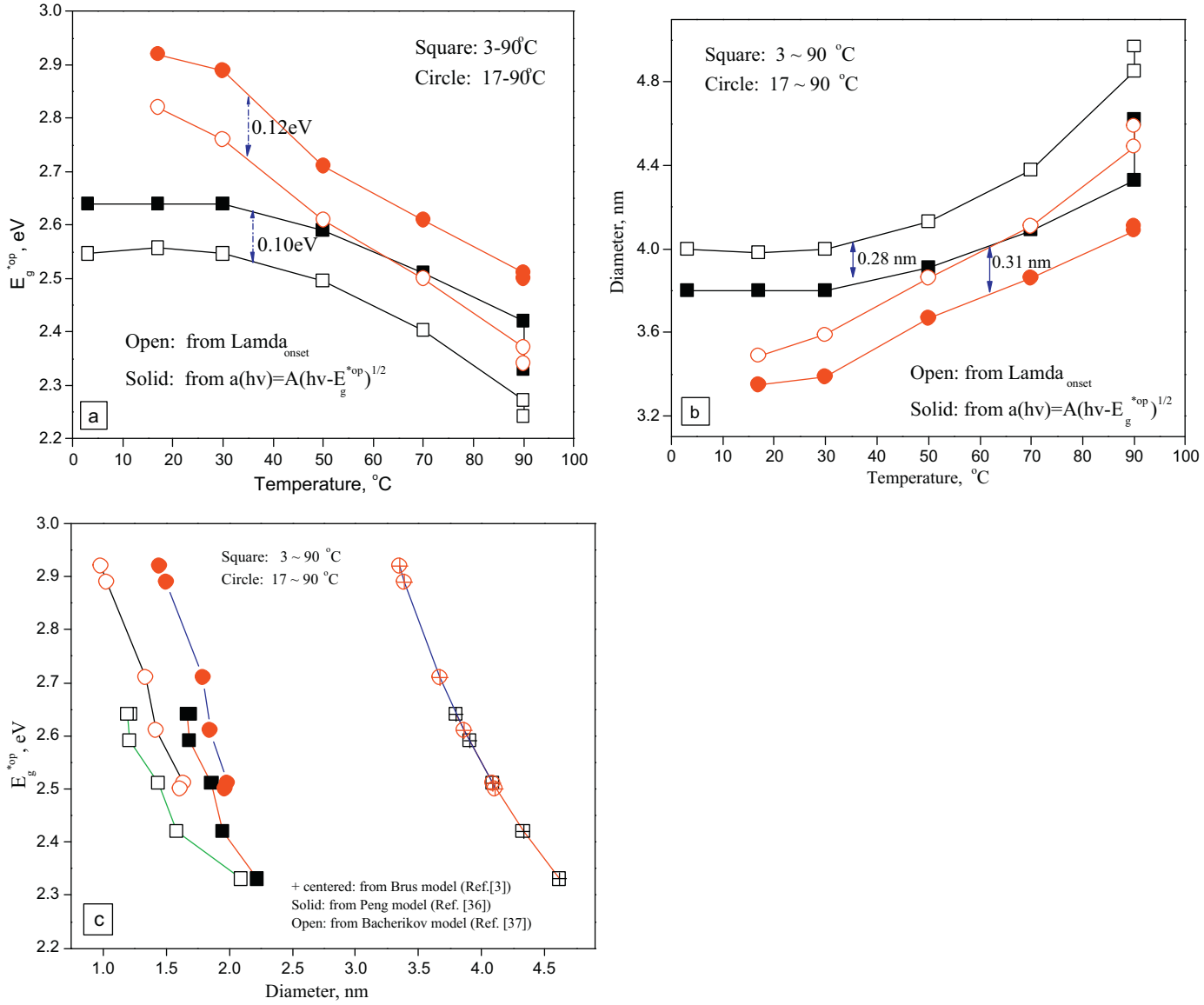

Fig. 6. Temperature dependences of the optical band gap (E_g^{*op}, a) and particle diameter (b) of the CdSe QDs. The relationships between E_g^{*op} and diameter both from this study and Refs. [36] and [37] were also shown in this figure (c).

Here the diameter results from λ_{onset} were not presented in this figure due to its low accuracy. As seen, similar decreasing tendencies of E_g^{*op} against particle diameter were observed for the CdSe QDs. The absolute values, however, were quite different. The calculated diameters from Ref. [37] were slightly smaller than those from Ref. [36]. And both were nearly half of the values from Brus model (see data in Table 1). We have carefully checked the Brus model as well as Eq. (4) to confirm that our calculations were correct, though some investigator confused the difference of radius and diameter for a particle [38]. Although the TEM observations gave a diameter value of 2–3 nm in this study (see Fig. 3b), a particle diameter size of ~2 nm would be most likely since it was inevitable that some very small nanoparticles, for instance particles with diameters less than 1 nm, have been missed in the TEM field. With this actual particle size, the model given in Ref. [36] was the most suitable one in this study for estimations of the particle size of the QDs while the Brus model gave quite large results. The reason was that the QDs in Brus model were assumed to be spherical and that the effective masses of charge carriers and the dielectric constant of the solid were constant as a function of size. As a result, this theoretical model mapped band gap and size well for larger QDs, for instance particles typically larger than ~8 nm in diameter while for those very small particles it did not work well [23,35].

3.5. Fluorescence spectra

The fluorescence performances of the synthesized CdSe QDs in this study were examined using a spectrofluorometer and the results were shown in Fig. 7. The absolute values of the photoluminescence (PL) intensities in Fig. 7 were much lower than those of CdSe/ZnS QDs [39]. This was due to the lack of ZnS shell. The excitation spectra were firstly recorded by using a detecting wavelength of 550 nm. The PL intensities of the spectra

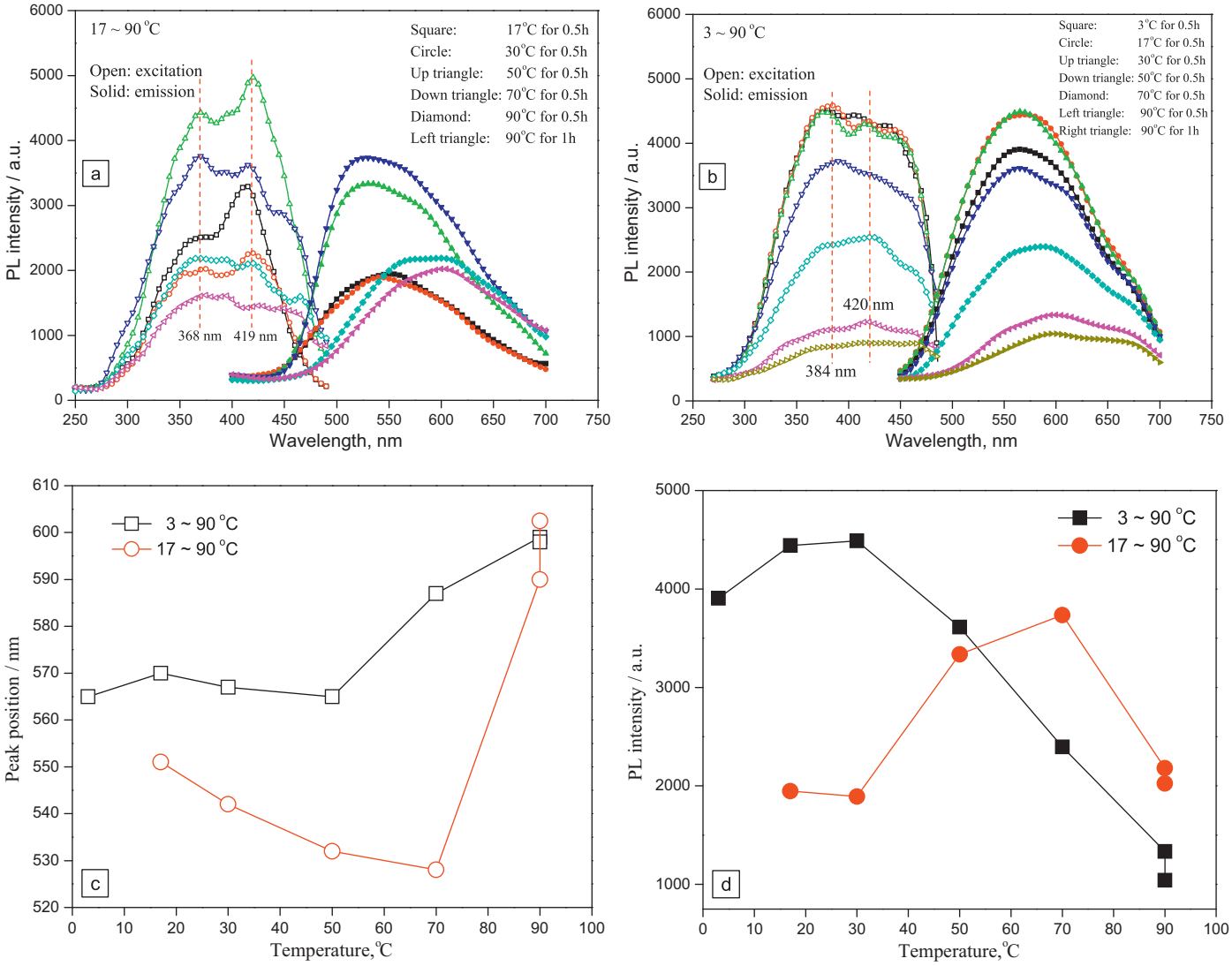

Fig. 7. Photoluminescence spectra of the CdSe QDs synthesized at a temperature range of 17–90 °C (a) and 3–90 °C (b). The detecting and exciting wavelengths were 550 nm and 365 nm, respectively. The peak position and intensity of the emission spectra were summarized in (c) and (d) for comparison.

significantly changed with the reaction temperature. Two typical peaks with peak positions of 368 nm and 419 nm were observed for the 17–90 °C samples while in the cases of the 3–90 °C samples they were at 384 nm and 420 nm (dash line in Fig. 7a).

With the above excitation results a 365 nm ultraviolet was used to excite the CdSe QDs and the obtained emission spectra were shown in Fig. 7a and b. The peak position and intensity were summarized and plotted in Fig. 7c and d for comparison. As seen, only one peak was observed. The peak position and intensity, however, significantly changed with the reaction temperature. For the 17–90 °C samples, with the raise of the reaction temperature the peak position linearly blue-shifted from 551 nm to 528 nm and then rapidly red-shifted to 602 nm. The PL intensity increased at the beginning, reached maximum at 70 °C, and then decreased. In the cases of the 3–90 °C samples both the peak position and intensity scarcely varied bellow 50 °C. For temperature above 50 °C, red shift of 565–598 nm was observed. The PL intensity over this temperature range linearly decreased. From a viewpoint of wide controls of fluorescence color and intensity, a reaction temperature range of 17–90 °C was appropriate for the synthesis of the CdSe QDs.

4. Conclusion

The CdSe QDs were synthesized at various temperatures in aqueous solution. The XRD examination did not give sharp diffraction peaks but rather flat humps and a Scherrer size range of 0.8–1.2 nm. The QDs were physically color gradient from pale green to orange and consisted of basically round particles with a particle size of ~2 nm in diameter. The SAED patterns of the QDs matched well with XRD examination, giving a visible shift of diffraction hump toward large angle. The UV–vis measurements revealed that the reaction temperature could significantly influence the band gap, particle size, and spectral behaviors of the QDs. With the increase of the synthesis temperature from room temperature to 90 °C, the band gap of the QDs noticeably decreased, corresponding to an essential increase of particle size as well as variable spectral behaviors. The starting temperature

dramatically had an important effect on the QDs synthesis and their optical properties. Both the peak position and intensity of the excitation and emission spectra significantly changed with the synthesis temperature. From a viewpoint of wide controls of fluorescence color and intensity, a reaction temperature range of 17–90 °C was appropriate for the synthesis of the CdSe QDs.

Acknowledgements

This work was financially supported by the Shandong Province Middle-aged and Young Scientists Research Incentive Fund (BS2009CL016), the Fundamental Research Funds for the Central Universities (201113002), and the National Natural Science Foundation of China (51172217).

References

[1] C. Zhang, Z.Y. Zhang, B.B. Yu, et al., Application of the biological conjugate between antibody and colloid AU nanoparticles as analysis to inductively coupled plasma mass spectrometry, Analytical Chemistry 74 (1) (2002) 96–99.
[2] L.E. Brus, A simple model for the ionization potential, electron affinity, and aqueous redox potentials of small semiconductor crystallites, Journal of Chemical Physics 79 (1983) 5566–5571.
[3] L.E. Brus, Electron–electron and electron–hole interactions in small semiconductor crystallites: the size dependence of the lowest excited electronic state, Journal of Chemical Physics 80 (1984) 4403–4409.
[4] Y. Wang, N. Herron, Quantum size effects on the exciton energy of CdS clusters, Physical Review B 42 (1990) 7253–7255.
[5] Y. Wang, N. Herron, Nanometer-sized semiconductor clusters: materials synthesis, quantum size effects, and photophysical properties, Journal of Physical Chemistry 95 (1991) 525–532.
[6] T. Trindade, P. O'Brien, Synthesis of CdS and CdSe nanocrystallites using a novel single-molecule precursors approach, Chemistry of Materials 9 (1997) 523–530.
[7] M.S. Seehra, P. Dutta, S. Neeleshwar, et al., Size-controlled ex-nihilo ferromag netism in capped CdSe quantum dots, Advanced Materials 20 (2008) 1656–1660.
[8] V.L. Colvin, M.C. Schlamp, A.P. Alivisatos, Light-emitting diodes made from cadmium selenide nanocrystals and a semiconducting polymer, Nature 370 (1994) 354–357.
[9] S. Coe, W.K. Woo, M. Bawendi, V. Bulovic, Electroluminescence from single monolayers of nanocrystals in molecular organic devices, Nature 420 (2002) 800–803.
[10] Q.J. Sun, Y.A. Wang, L.S. Li, et al., Bright, multicoloured light-emitting diodes based on quantum dots, Nature Photonics 1 (2007) 717–722.
[11] N.C. Greenham, X.G. Peng, A.P. Alivisatos, Charge separation and transport in conjugated-polymer/semiconductor nanocrystal composites studied by photoluminescence quenching and photoconductivity, Physical Review B 54 (1996) 17628–17637.
[12] W.U. Huynh, X.G. Peng, A.P. Alivisatos, CdSe nanocrystal rods/poly (3-hexylthiophene) composite photovoltaic devices, Advanced Materials 11 (1999) 923–927.
[13] C.W. Chan Warren, S.M. Nie, Quantum dot bioconjugates for ultrasensitive nonisotopic detection, Science 281 (1998) 2016–2018.
[14] M. Bruchez, M. Moronne, P. Gin, S. Weiss, A.P. Alivisatos, Semiconductor nanocrystals as fluorescent biological labels, Science 281 (1998) 2013–2016.
[15] H. Mattoussi, J.M. Mauro, E.R. Goldman, G.P. Anderson, V.C. Sundar, F.V. Mikulec, M.G. Bawendi, Self-assembly of CdSe–ZnS quantum dot bioconjugates using an engineered recombinant protein, Journal of the American Chemical Society 122 (2000) 12142–12150.
[16] X. Peng, M.C. Schlamp, A.V. Kadavanich, A.P. Alivisatos, Epitaxial growth of highly luminescent CdSe/CdS core/shell nanocrystals with photostability and electronic accessibility, Journal of the American Chemical Society 119 (1997) 7019–7029.
[17] S. Kim, B. Fisher, H.J. Eisler, M. Bawendi, Type-II quantum dots: CdTe/CdSe (core/shell) and CdSe/ZnTe (core/shell) heterostructures, Journal of the American Chemical Society 125 (2003) 11466–11467.
[18] N. Gaponik, D.V. Talapin, A.L. Rogach, K. Hoppe, E.V. Shevchenko, A. Kornowski, A. Eychmuller, H. Weller, Thiol-capping of CdTe nanocrystals: an alternative to organometallic synthetic routes, Journal of Physical Chemistry B 106 (2002) 7177–7185.
[19] H. Li, W.Y. Shih, W.H. Shih, Synthesis and characterization of aqueous carboxyl-capped CdS quantum dots for bioapplications, Industrial and Engineering Chemistry Research 46 (2007) 2013–2019.
[20] H. Li, W.Y. Shih, W.H. Shih, Non-heavy-metal ZnS quantum dots with bright blue photoluminescence by a one-step aqueous synthesis, Nanotechnology 18 (2007) 205604.
[21] A.L. Rogach, A. Kornowski, M. Gao, A. Eychmuller, H. Weller, Synthesis and characterization of a size series of extremely small thiol-stabilized CdSe nanocrystals, Journal of Physical Chemistry B 103 (1999) 3065–3069.
[22] J.J. Liu, Z.X. Shi, Y.C. Yu, R.Q. Yang, S.L. Zuo, Water-soluble multicolored fluorescent CdTe quantum dots: synthesis and application for fingerprint developing, Journal of Colloid and Interface Science 342 (2010) 278–282.
[23] L.E. Brus, Electronic wave functions in semiconductor clusters: experiment and theory, Journal of Physical Chemistry 90 (1986) 2555–2560.
[24] X.G. Peng, L. Manna, W.D. Yang, J. Wickham, E. Scher, A. Kadavanich, A.P. Alivisatos, Shape control of CdSe nanocrystals, Nature 404 (2000) 59–61.
[25] Z.A. Peng, X.G. Peng, Mechanisms of the shape evolution of CdSe nanocrystals, Journal of the American Chemical Society 123 (2001) 1389–1395.
[26] L. Manna, E.C. Scher, A.P. Alivisatos, Synthesis of soluble and processable rod-, arrow-, teardrop-, and tetrapod-shaped CdSe nanocrystals, Journal of the American Chemical Society 122 (2000) 12700–12706.
[27] X.G. Peng, J. Wickham, A.P. Alivisatos, Kinetics of II–VI and III–V colloidal semiconductor nanocrystal growth: focusing of size distributions, Journal of the American Chemical Society 120 (1998) 5343–5344.
[28] C.B. Murray, D.J. Norris, M.G. Bawendi, Synthesis and characterization of nearly monodisperse CdE (E- S, Se,Te) semiconductor nanocrystals, Journal of the American Chemical Society 115 (1993) 8706–8715.
[29] D.L. Klayman, T.S. Griffin, Reaction of selenium with sodium borohydride in protic solvents: a facile method for the introduction of selenium into organic molecules, Journal of the American Chemical Society 95 (l) (1973) 197–199.
[30] M.T. Weller, Inorganic Materials Chemistry, Oxford University Press, Oxford, 1997.
[31] K. Colladet, M. Nicolas, L. Goris, L. Lutsen, D. Vanderzande, Low-band gap polymers for photovoltaic applications, Thin Solid Films 451–452 (2004) 7–11.
[32] J.I. Pankove, Optical Processes in Semiconductors, Dover Publications Inc., New York, 1970.
[33] M.L. Steigerwald, L.E. Brus, Semiconductor crystallites: a class of large molecules, Accounts of Chemical Research 23 (1990) 183–188.
[34] L.I. Berger, Semiconductor Materials, CRC Press, Boca Raton, FL, 1997
[35] E. Hendry, M. Koeberg, F. Wang, H. Zhang, C.M. Donega, D. Vanmaekelbergh, M. Bonn, Direct observation of electron-to-hole energy transfer in CdSe quantum dots, Physical Review Letters 96 (2006) 057408.
[36] W.W. Yu, L. Qu, W. Guo, X.G. Peng, Experimental determination of the extinction coefficient of CdTe, CdSe, and CdS nanocrystals, Chemistry of Materials 15 (2003) 2854–2860.
[37] Y. Bacherikov, M.O. Davydenko, A.M. Dmytruk, I.M. Dmitruk, P.M. Lytvyn, I.V. Prokopenko, R. Romanyuk, Semiconductor Physics, Quantum Electronics and Optoelectronics 9 (2006) 75.
[38] K. Koc, F.Z. Tepehan, G.G. Tepehan, Characterization of MPS capped CdS quantum dots and formation of self-assembled quantum dots thin film on a glassy substrate, Chalcogenide Letters 8 (4) (2011) 239–247.
[39] B.O. Dabbousi, J. Rodriguez-Viejo, F.V. Mikulec, R.J. Heine, H. Mattoussi, R. Ober, K.F. Jensen, M.G. Bawendi, (CdSe)ZnS core-shell quantum dots: synthesis and optical and structural characterization of a size series of highly luminescent materials, Journal of Physical Chemistry B 10 (1997) 9463–9475.